ORIGINAL RESEARCH

Fibroblast Growth Factor Signaling Mediates Pulmonary Endothelial Glycocalyx Reconstitution

Yimu Yang[1], Sarah M. Haeger[1], Matthew A. Suflita[2], Fuming Zhang[3], Kyrie L. Dailey[1], James F. Colbert[1], Joshay A. Ford[1], Mario A. Picon[1], Robert S. Stearman[4], Lei Lin[3], Xinyue Liu[3], Xiaorui Han[3], Robert J. Linhardt[3], and Eric P. Schmidt[1,5]

[1]Department of Medicine, University of Colorado Denver, Aurora, Colorado; Departments of [2]Biology and [3]Chemistry, Rensselaer Polytechnic Institute, Troy, New York; [4]Department of Medicine, Indiana University School of Medicine, Indianapolis, Indiana; and [5]Department of Medicine, Denver Health Medical Center, Denver, Colorado

Abstract

The endothelial glycocalyx is a heparan sulfate (HS)–rich endovascular structure critical to endothelial function. Accordingly, endothelial glycocalyx degradation during sepsis contributes to tissue edema and organ injury. We determined the endogenous mechanisms governing pulmonary endothelial glycocalyx reconstitution, and if these reparative mechanisms are impaired during sepsis. We performed intravital microscopy of wild-type and transgenic mice to determine the rapidity of pulmonary endothelial glycocalyx reconstitution after nonseptic (heparinase-III mediated) or septic (cecal ligation and puncture mediated) endothelial glycocalyx degradation. We used mass spectrometry, surface plasmon resonance, and *in vitro* studies of human and mouse samples to determine the structure of HS fragments released during glycocalyx degradation and their impact on fibroblast growth factor receptor (FGFR) 1 signaling, a mediator of endothelial repair. Homeostatic pulmonary endothelial glycocalyx reconstitution occurred rapidly after nonseptic degradation and was associated with induction of the HS biosynthetic enzyme, exostosin (EXT)-1. In contrast, sepsis was characterized by loss of pulmonary EXT1 expression and delayed glycocalyx reconstitution. Rapid glycocalyx recovery after nonseptic degradation was dependent upon induction of FGFR1 expression and was augmented by FGF-promoting effects of circulating HS fragments released during glycocalyx degradation. Although sepsis-released HS fragments maintained this ability to activate FGFR1, sepsis was associated with the downstream absence of reparative pulmonary endothelial FGFR1 induction. Sepsis may cause vascular injury not only via glycocalyx degradation, but also by impairing FGFR1/EXT1–mediated glycocalyx reconstitution.

Keywords: sepsis; fibroblast growth factor; heparan sulfate

Clinical Relevance

The endothelial glycocalyx is a heparan sulfate–rich endovascular layer critical to endothelial function. Accordingly, sepsis-associated degradation of the pulmonary endothelial glycocalyx contributes to septic lung injury; however, little is understood about the mechanisms governing glycocalyx reconstitution or their fate during sepsis. Using animal and human studies, we demonstrate that fibroblast growth factor receptor 1/exostosin 1 signaling is necessary for glycocalyx reconstitution and that these homeostatic processes are impaired during sepsis.

(Received in original form October 25, 2016; accepted in final form January 13, 2017)

This work was supported by NHLBI R01 HL125371 (R.J.L. and E.P.S.).

Author Contributions: Y.Y. performed intravital microscopy and animal models of sepsis, contributed to experimental design, and assisted with manuscript preparation; S.M.H. and J.F.C. performed micro-RNA-16 studies and contributed to experimental design; M.A.S. performed Baf3 analyses; F.Z. performed surface plasmon resonance experiments; K.L.D., M.A.P., and R.S.S. performed *in vitro* endothelial studies; J.A.F. coordinated animal breeding and *in vivo* experiments; L.L., X.L., and X.H. performed heparan sulfate analyses; R.J.L. supervised BaF3, surface plasmon resonance, and mass spectrometry, contributed to experimental design, and assisted with manuscript preparation; E.P.S. designed experiments, performed statistical analyses, supervised the project, and wrote the manuscript.

Correspondence and requests for reprints should be addressed to Eric P. Schmidt, M.D., 12700 East 19th Avenue, Research Complex 2, Mail Stop C272, Aurora, CO 80045. E-mail: eric.schmidt@ucdenver.edu

This article has an online supplement, which is accessible from this issue's table of contents at www.atsjournals.org

Am J Respir Cell Mol Biol Vol 56, Iss 6, pp 727–737, Jun 2017

Originally Published in Press as DOI: 10.1165/rcmb.2016-0338OC on February 10, 2017
Internet address: www.atsjournals.org

The endothelial glycocalyx is a heparan sulfate (HS)–rich layer of glycosaminoglycans and associated proteoglycans that lines the micro- and macrovascular intima. *In vivo*, glycocalyx glycosaminoglycans become highly hydrated, forming a substantial gel-like endothelial surface layer (ESL) that projects 0.5 μm to over 10 μm into the vascular lumen (1). An intact ESL contributes to the endothelial barrier to fluid and protein, regulates leukocyte–endothelial adhesion, and transduces fluid shear stress into endothelial nitric oxide synthesis (2). Accordingly, a number of acute and chronic vascular diseases are characterized by degradation of the glycocalyx/ESL (collectively referred to subsequently here as the "ESL"). For example, rapid induction of endothelial heparanase (a TNF-α–activated, HS-specific mammalian endoglucuronosyl hydrolase) degrades ESL HS during sepsis, leading to lung (3) and kidney (4) injury.

Given the importance of ESL integrity to vascular homeostasis, endothelial cells would be expected to rapidly repair a damaged ESL. However, little is known about the endogenous mechanisms driving ESL reconstitution. Mouse cremasteric ESL recovery occurred within 5 days of intravenous heparinase-III (a bacterial HS-specific endoglucuronosyl lyase) or intrascrotal TNF-α (5). It is unclear if a similarly slow pace of ESL recovery occurs within the lung, an organ characterized by a thicker ESL (3) and greater functional susceptibility to edema. Indeed, *in vitro* studies of endothelial cells under shear stress demonstrate that glycocalyx recovery is capable of occurring as rapidly as 12 hours after enzymatic HS degradation (6).

As HS is a critical contributor to ESL structure and function (3), ESL reconstitution likely requires induction of HS biosynthesis. HS is a linear glycosaminoglycan composed of repeating hexuronic acid-glucosamine disaccharides, the polymerization of which is dependent upon glucosyltransferases, such as exostosin (EXT)-1 (2). After polymerization, HS undergoes targeted epimerization and sulfation, yielding highly sulfated regions (at least five saccharides in length) of sufficiently negative charge to interact with positively charged residues of proteins, including growth factor ligands and their cognate receptors. Through these charge-based interactions, HS can serve as a scaffolding molecule, facilitating growth factor ligand–receptor binding and promoting downstream signaling (2).

We hypothesized that pulmonary ESL reconstitution would occur rapidly after (nonseptic) HS degradation with heparinase-III, reflecting the critical homeostatic functions of an intact pulmonary ESL. We hypothesized that ESL repair would be promoted by activation of endothelial growth factor signaling by highly sulfated HS fragments released into the circulation during ESL degradation. Finally, we hypothesized that these homeostatic processes of ESL reconstitution would be impaired during sepsis, suggesting that septic vascular dysfunction may arise not only from ESL degradation, but also from delayed reconstitution.

Materials and Methods

Cell Culture

In vitro experiments were performed as described in the online supplemental Materials and Methods.

Animals

Experiments were approved by the University of Colorado Denver (Aurora, CO) Institutional Animal Care and Use Committee and conducted in accordance with National Institutes of Health (Bethesda, MD) guidelines. Wild-type male C57BL/6 mice (8–10 wk old) were purchased from Jackson (Bar Harbor, ME). Endothelial-specific *Fgfr1/2* knockout mice (Tie2-Cre:*Fgfr1/2*$^{f/f}$) were generously provided by Dr. David Ornitz (Washington University in St. Louis, St. Louis, MO) (7). Additional details are provided in the online supplemental Materials and Methods.

Human Subjects

As previously described (3, 8), we prospectively obtained plasma samples from mechanically ventilated patients with nonpulmonary sepsis or pneumonia within 72 hours of admission to the Denver Health Medical Center Medical Intensive Care Unit (ClinicalTrials.gov NCT009380002). We obtained written, informed consent from patients' proxy decision makers before plasma collection. The Colorado Multiple Institutions Review Board (Aurora, CO) approved all protocols.

Induction of Murine Sepsis

We induced sepsis in 8- to 12-week-old male C57BL/6 mice by cecal ligation and puncture (CLP), as previously described (3) and detailed in the online supplemental Materials and Methods.

Measurement of Pulmonary ESL Thickness

As previously described (3, 9), we measured pulmonary ESL thickness by dextran exclusion using closed-chest intravital microscopy of the mouse subpleural microvasculature. For determination of ESL recovery after nonseptic degradation, we administered a one-time dose of intravenous heparinase-III (1 [Sigma] unit; Sigma-Aldrich, St. Louis, MO) or heat-inactivated heparinase-III (1 unit, boiled for 15 min) and measured ESL thickness via dextran exclusion 24 hours later. For determination of ESL recovery after sepsis, we performed CLP and then performed intravital microscopy of the subpleural microcirculation 24, 48, or 72 hours later. Additional details are provided in the online supplemental Materials and Methods.

Plasma HS Isolation and Quantification

HS was isolated from the plasma of patients with nonpulmonary sepsis (pooled from four subjects) or pneumonia (five subjects) as previously described (8), and disaccharide analyses were performed via liquid chromatography–tandem mass spectrometry, as detailed in the online supplemental Materials and Methods. Plasma HS fragment size was determined via PAGE with Alcian blue/silver staining, as described in the online supplemental Materials and Methods.

Surface Plasmon Resonance

The binding of HS oligosaccharides to FGF2 was determined using surface plasmon resonance (SPR). FGF2–HS binding was measured by the ability of exogenous HS oligosaccharides (of various sizes; sulfation) to interfere with FGF2 binding to heparin immobilized on a SPR chip, as detailed in the online supplemental Materials and Methods.

BaF3 Signaling Assay

We treated BaF3 cells expressing FGFR1c (the nonepithelial FGFR1 isoform [10]) with FGF2 (5 nmol/l), FGF1 (5 nmol/l), or

HS oligosaccharides/fragments (various concentrations), and measured optical density to determine the impact of HS oligosaccharides on FGF2–FGFR1 signaling. Alternatively, we treated cells with FGF2 (5 nmol/l) and HS fragments isolated from pooled human plasma (250 ng/ml). As these cells are dependent on FGFR1c for survival, cell density directly reflects FGFR1c activity, as previously described (11).

Statistical Analyses

Animals were randomized to treatment or control groups. Experimental replicates were performed on the same day as a matching control. Single comparisons were made using Student's two-tailed *t* test. Multiple comparisons were made by ANOVA with Tukey's *post hoc* analysis. Results were considered statistically significant at a P value less than 0.05. All graphs demonstrate mean values (±SE). Analyses were performed using Prism (GraphPad Software Inc., La Jolla, CA).

Results

Homeostatic Pulmonary ESL Reconstitution Occurs Rapidly after Heparinase-III–Mediated Degradation, but Is Delayed after Sepsis-Associated Degradation

The pulmonary ESL is a substantial endovascular structure with HS-dependent size and function (3). To determine the mechanisms underlying ESL recovery after nonseptic HS degradation, we treated mice with intravenous heparinase-III, an HS-specific endoglucuronosyl lyase that rapidly degrades the pulmonary ESL (3, 12). Using our previously established, intravital microscopy–based dextran exclusion technique (9), we observed that the pulmonary ESL is completely reconstituted within 24 hours of heparinase-III–mediated degradation (Figure 1A). This rapid ESL reconstitution coincided with induction of pulmonary EXT1, an enzyme necessary for HS polymerization (13). The increase in lung homogenate EXT1 protein (Figure 1B) occurred before a statistically significant increase in lung homogenate EXT1 mRNA (Figure 1C), potentially reflecting both transcriptional and post-transcriptional control of EXT1 expression. HS synthesis was necessary to pulmonary ESL recovery, as timely reconstitution did not occur in mice treated with the artificial glycan 4-fluoro-*N*-acetyl-glucosamine (4-F-GlcNAc; Figure 1D), which interrupts EXT1-mediated HS polymerization (14, 15). Although heparinase-III alone was insufficient to induce lung edema 6 hours (wet:dry ratio = 4.42 ± 0.25 in heparinase-III–treated wild-type mice; 4.40 ± 0.52 in heat-inactivated heparinase-III–treated wild-type mice; $n = 4$; $P = 0.96$) or 24 hours (Figure 1E) after injection, heparinase-III treatment followed 6 hours later by 4-F-GlcNAc–mediated inhibition of HS polymerization induced pulmonary edema at 24 hours (Figure 1E), demonstrating that processes of pulmonary ESL recovery are homeostatic.

After determining the rapidity of homeostatic pulmonary ESL reconstitution after nonseptic degradation, we sought to determine if similar recovery occurs during sepsis. We have previously demonstrated that sepsis (as modeled in mice using CLP) induces expression of mammalian heparanase, an enzyme that degrades pulmonary ESL thickness with similar rapidity (i.e., <30 min) as heparinase-III (3). Despite similar rapidity of degradation, pulmonary ESL reconstitution after CLP was significantly delayed (72 h, Figure 1F) in comparison to heparinase-III (24 h, Figure 1A). Administration of the heparanase inhibitor, *N*-desulfated, re-*N*-acetylated heparin, after septic ESL degradation did not accelerate ESL reconstitution (Figure 1F), suggesting that delayed ESL reconstitution during sepsis was not simply due to ongoing degradation, but instead reflected aberrant ESL repair. Indeed, CLP-treated mice demonstrated an early loss of pulmonary EXT1 expression (Figures 1G and 1H), contrasting EXT1 induction observed after heparinase-III (Figures 1B and 1C). CLP-treated mice eventually demonstrated return of baseline pulmonary EXT1 expression (Figure 1H), coincident with ESL recovery. CLP-treated mice had no evidence of compensatory induction of pulmonary EXT2 or EXT-like 2, salvage HS polymerases previously noted (16) to produce (albeit truncated) HS in EXT1-deficient cells (*see* Figure E1 of the online supplement).

FGFR1 Mediates Pulmonary ESL Reconstitution after Heparinase-III, but Is Suppressed after CLP

To determine the mechanisms underlying delayed pulmonary ESL reconstitution during sepsis, we first sought to define the mechanisms responsible for rapid pulmonary ESL reconstitution after heparinase-III. Recent reports have implicated fibroblast growth factor (FGF) receptors (FGFRs) in endothelial recovery after vascular injury (7). FGFR1 is the predominant FGFR expressed in pulmonary endothelial cells (Figure E2, as well as a review of publically available RNA sequencing data [17]). Accordingly, heparinase-III–mediated ESL degradation was followed by increased pulmonary FGFR1 expression (Figure 2A). Pulmonary endothelial FGFR1 induction after heparinase-III was ESL reparative, as Tie2-Cre *Fgfr1/2*$^{f/f}$ mice (which lack endothelial FGFR1 [7]; Figure E3) demonstrated absence of pulmonary EXT1 induction (Figure 2B) and delayed ESL reconstitution (Figure 2C) after heparinase-III. These transgenic investigations were complemented by experiments using AZD4547, a high-affinity FGFR1 inhibitor (18) (Figures 2D and 2E). Similar to 4-F-GlcNAc (Figure 1E), AZD4547-induced impairment of ESL reconstitution induced lung edema, again suggesting that FGFR1/EXT1–mediated ESL reconstitution was homeostatic (*see* Figure E4). However, this partial impairment in reconstitution was not sufficient to cause lung edema in Tie2-Cre *Fgfr1/2*$^{f/f}$ mice, suggesting the presence of compensatory lung-protective pathways in these mice constitutively lacking endothelial FGFR1 signaling.

In contrast to the reparative induction of FGFR1 in wild-type mice after heparinase-III–mediated ESL degradation, FGFR1 expression was suppressed after CLP-mediated ESL degradation (Figure 3A). To determine if this septic loss of FGFR1 expression occurred within the pulmonary endothelium, we treated primary mouse lung microvascular endothelial cells with LPS and observed decreased endothelial FGFR1 expression (Figure 3B).

Previous studies have demonstrated that endothelial FGFR1 expression can be decreased by micro-RNA (miR)-16 (19), an endothelial-expressed miR previously observed in the plasma of humans (20) and animals (21) with sepsis. We similarly noted a trend ($P = 0.09$) toward increased plasma miR-16 12 hours after CLP (Figure E5). However, pulmonary miR-16 expression was decreased 3 hours after CLP (Figure 3C), suggesting that miR-16 was unlikely to be active in the lung concurrent with CLP-induced loss of pulmonary

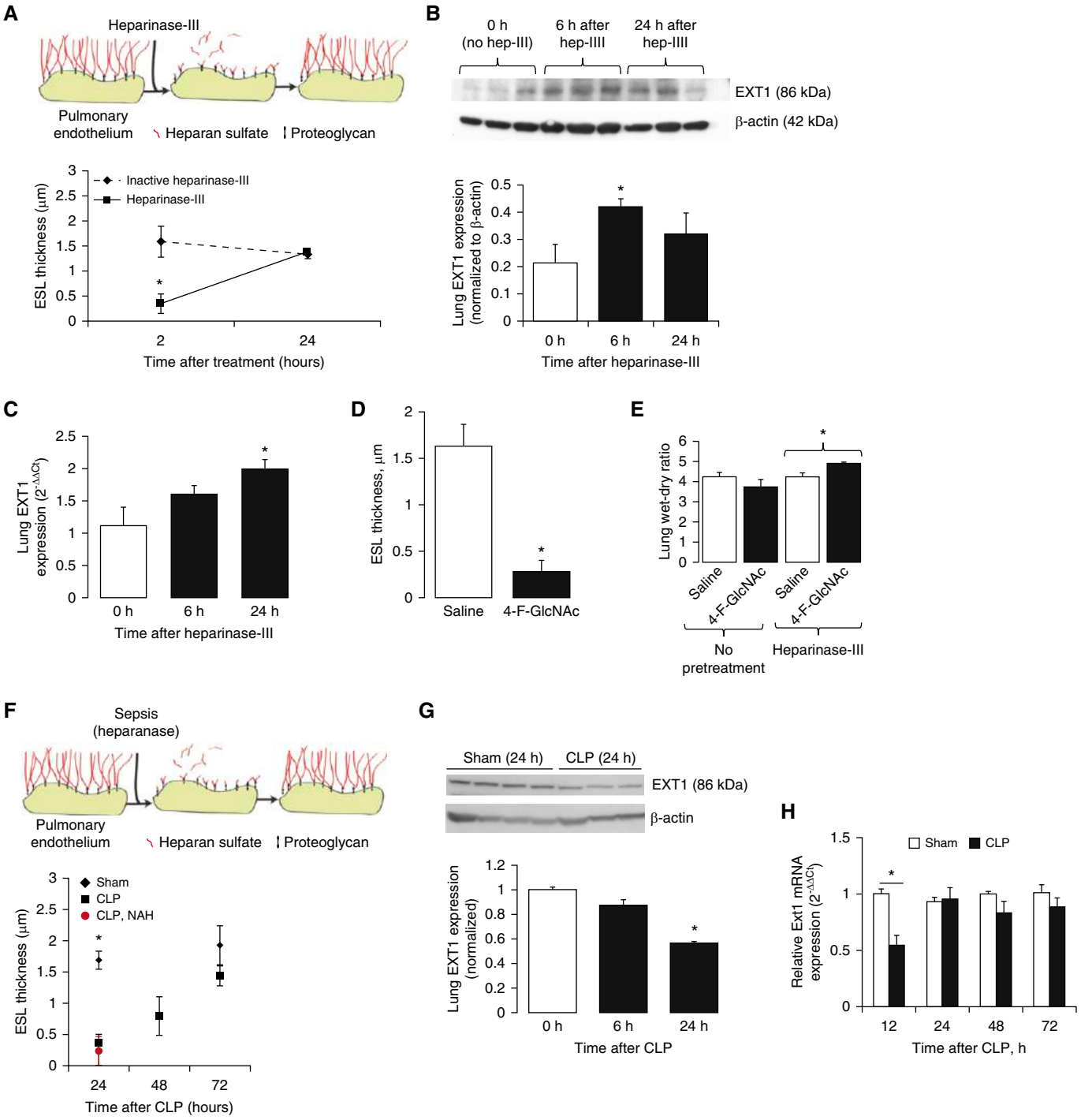

Figure 1. Homeostatic pulmonary endothelial surface layer (ESL) reconstitution occurs rapidly after heparinase (hep)-III–mediated degradation but slowly after sepsis-mediated degradation. (*A*) Thickness of the heparan sulfate (HS)–rich pulmonary ESL (measured via intravital microscopy) rapidly declines after nonseptic degradation (heparinase-III, 1 unit intravenous) but recovers within 24 hours. Lungs from heparinase-III–treated mice demonstrated increased protein (*B*) and mRNA (*C*) expression of exostosin (EXT)-1, a glucosyltransferase required for HS synthesis. EXT1 is necessary for homeostatic ESL reconstitution, as inhibition of EXT1 activity after heparinase-III–mediated ESL degradation (4-fluoro-*N*-acetyl-glucosamine [4-F-GlcNAc], 2.5 mg intraperitoneally 6, 12, and 18 h after heparinase-III) delayed ESL recovery (*D*) and induced lung edema (*E*) 24 hours after ESL degradation. In contrast to heparinase-III, cecal ligation and puncture (CLP)–induced ESL degradation (a process mediated by heparanase, a mammalian heparinase-III analog) is delayed (*F*). ESL recovery 24 hours after CLP is not accelerated by heparanase inhibition (150 μg *N*-desulfated, re-*N*-acetylated heparin [NAH]) administered subcutaneously 6, 12, and 18 hours after CLP, indicating that delayed reconstitution is not a function of ongoing septic HS degradation. Consistent with impaired ESL recovery, lungs from CLP-treated mice demonstrated decreased EXT1 protein (*G*) and mRNA (*H*) expression. $n > 3$ per group, $^*P < 0.05$. All graphs demonstrate mean values (±SE).

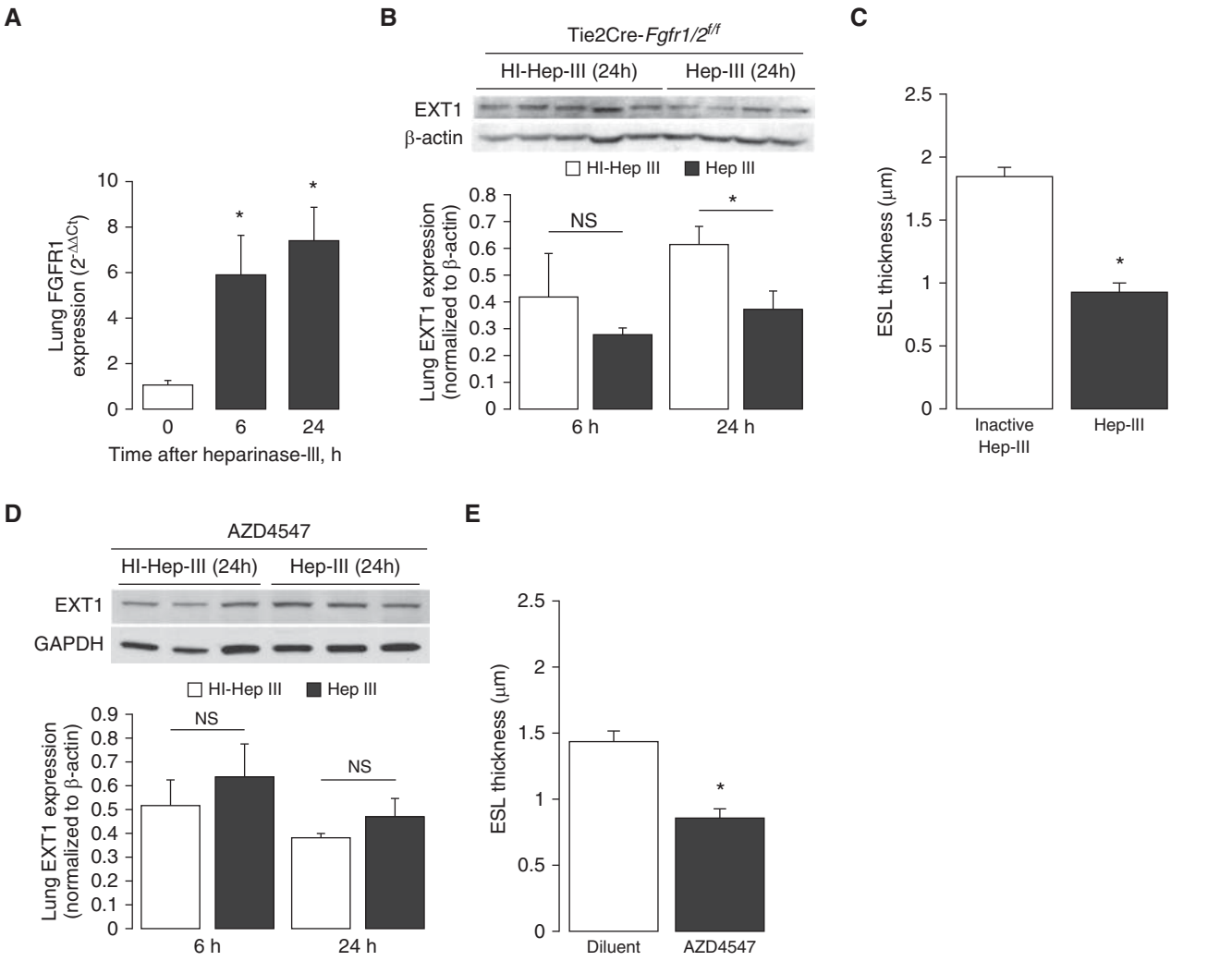

Figure 2. Fibroblast growth factor receptor (FGFR) 1 signaling mediates EXT1 expression and ESL reconstitution after heparinase-III. (*A*) Heparinase-III treatment (1 unit intravenous at time = 0) induces pulmonary expression of FGFR1 within wild-type C57BL/6 mice. (*B*) Tie2Cre-*Fgfr1/2*$^{f/f}$ mice, which feature loss of pulmonary endothelial FGFR1, demonstrated loss of EXT1 expression after heparinase-III (1 unit intravenous [*B*]) and, accordingly, delayed 24 hours ESL recovery (*C*) in comparison to heat-inactivated heparinase-III (HI-Hep-III). Western blot images (*B* and *D*) demonstrate one mouse per lane. Pretreatment of wild-type C57BL/6 mice with the FGFR1 inhibitor AZD45457 (12.5 μg/g body weight by gavage 3 h before heparinase-III) similarly prevented EXT1 induction (*D*) and delayed 24-hour ESL reconstitution (*E*). $n > 3$ per group; $^*P < 0.05$. NS, not significant. All graphs demonstrate mean values (±SE).

FGFR1 (Figure 3A). Furthermore, treatment of mice with an miR-16 blocking oligonucleotide had no impact on pulmonary expression of EXT1 (Figure 3D) 12 hours after CLP, indicating that septic loss of pulmonary EXT1 occurred in an miR-16–independent fashion.

HS Fragments Released after Heparinase-III–Mediated ESL Degradation Activate FGFR1 Signaling

In human diseases characterized by ESL degradation, HS fragments are released into the circulation (22). We previously observed (8) that these plasma HS fragments include hexasaccharides to octasaccharides (degree of polymerization [dp] 6 to dp8) as well as larger-weight fractions, with high degrees of glucosamine amino-sulfation (*N*-sulfated, Figure 4A). These structural characteristics suggest that circulating HS fragments are capable of influencing growth factor signaling, as they meet typical size and sulfation requirements necessary for interaction with positively charged residues of growth factor ligands and their cognate receptors (2, 10).

We therefore sought to determine if heparinase-III–mediated ESL degradation in mice similarly released highly sulfated HS fragments capable of regulating endothelial-reparative FGFR1 signaling. Treatment of mice with heparinase-III was associated with increased plasma *N*-sulfated HS fragments (as measured by mass spectrometry, Figure 4B and Figure E6) in a time course consistent with loss of ESL thickness (Figure 1A). As measurement of HS fragment size in mouse plasma is technically infeasible (given low plasma concentrations and small sample volumes), we instead isolated HS from whole mouse lungs, then treated extracted HS *ex vivo* with heparinase-III and performed gel

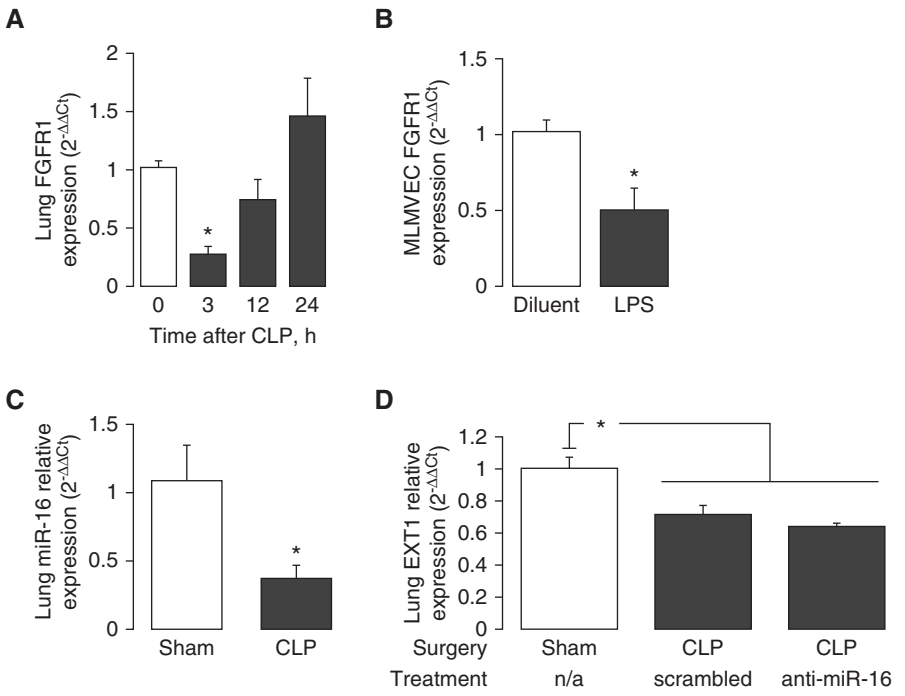

Figure 3. Sepsis is associated with suppression of pulmonary FGFR1. (*A*) In contrast to heparinase-III treatment, CLP was associated with loss of pulmonary FGFR1 expression. (*B*) Mouse lung microvascular endothelial cells (MLMVECs) similarly demonstrated diminished FGFR1 mRNA 6 hours after LPS treatment (10 μg/ml × 45 min, followed by media change). (*C*) Expression of microRNA (miR)-16 (a sepsis-associated miR that suppresses FGFR1) was decreased within the lung 3 hours after CLP, a time point characterized by maximal FGFR1 suppression; expression normalized to sham and housekeeping miR103 ($2^{-\Delta\Delta Ct}$). (*D*) Accordingly, antagonism of miR-16 with an anti-miR (5 μg/g body weight intraperitoneally, given 12 hours before CLP) had no effect on EXT1 expression 12 hours after CLP. Similar findings were noted with 25 μg/g anti-miR dosing (data not shown). $n > 3$ per group; $^*P < 0.05$ compared with sham/diluent/untreated control. All graphs demonstrate mean values (±SE). n/a, not applicable.

electrophoresis. The vast majority of lung HS fragments yielded after heparinase-III treatment were dp6 or larger in size (Figure 4C).

We next determined if highly sulfated HS fragments larger than dp6 can influence endothelial FGFR1 signaling. Using SPR, we examined the ability of HS to interact with FGF2, an FGFR1 ligand constitutively expressed within the lung (23) and implicated in endothelial repair (7, 19). FGF2 avidly bound to full-length glycosaminoglycans with high concentrations of *N*-sulfated glucosamines (Figure 5A), suggesting that *N*-sulfation was important for FGF2 binding. The necessity of *N*-sulfation in FGF2 binding was confirmed by selectively *N*-desulfating heparin, which dramatically attenuated FGF2 binding (Figure 5B). FGF2–HS interactions were additionally size dependent, with only fragments larger than dp6 in size having substantial binding (Figure 5C). Together, these findings indicate that circulating HS fragments released during heparinase-III–mediated ESL degradation are of sufficient size and sulfation to bind to FGF2.

To determine the impact of HS fragment–FGF2 binding on FGFR1 signaling, we used BaF3 cells stably transfected with FGFR1c, the primary FGF2 receptor splice variant expressed in pulmonary endothelial cells (Figure E2 [10, 17]). These cells require FGFR1 activation to grow/survive, as quantified by optical density. FGF2-induced BaF3 cell survival/growth was significantly augmented (Figure 5D) by the addition of highly sulfated heparin or HS octasaccharides (representative of >dp6 fragments released after heparinase-III). FGFR1c activation occurred at similar octasaccharide concentrations as those observed in the plasma of heparinase-III–treated mice (~50 ng/ml *N*-sulfated HS, per Figure 4B, approximated in BaF3 experiments by similar concentrations of highly sulfated heparin oligosaccharides). Heparin or HS octasaccharides were incapable of activating FGFR1c in the absence of FGF2 (Figure E7). We confirmed activation of endothelial FGFR signaling by measuring FGFR induction of extracellular signal–regulated kinase signaling (19) in HPMVEC-1.6R cells (a human pulmonary microvascular endothelial cells line [24], Figures 6A and 6C) treated with dp8 HS and FGF2. FGFR dependence of extracellular signal–regulated kinase activation was confirmed by pretreatment with AZD4547 (Figures 6B and 6C).

HS/FGF2 treatment of HPMEC-ST1.6R cells (Figure 6D) or primary mouse lung microvascular endothelial cells (Figure 6E) significantly induced EXT1 expression in an FGFR-dependent fashion (Figure 6D). Taken together with the absence of EXT1 induction in FGFR-inhibited mice (Figures 2B and 2D), these findings suggest that HS fragments, released during heparinase-III–mediated ESL degradation, activate endothelial FGF2/FGFR1 signaling and promote EXT1-mediated ESL reconstitution.

HS Fragments Released after CLP-Mediated ESL Degradation Activate FGFR1 Signaling

Given the observed loss of pulmonary EXT1 induction and delay in ESL reconstitution after CLP, we sought to determine if sepsis was associated not only with loss of reparative endothelial FGFR1 expression (Figure 3A), but also impaired FGFR1 activation by circulating HS fragments. Similar to heparinase-III treatment, CLP-treated mice demonstrated increased circulating *N*-sulfated HS fragments (Figure 7A) in concentrations sufficient to induce FGFR1c signaling in BaF3 cells (Figure 5D). Furthermore, there was an abundance of pulmonary FGF2 during sepsis (Figure 7B). We treated BaF3 cells with HS fragments (dp6–dp8 oligosaccharides or larger [8]) pooled from plasma of human patients with sepsis to confirm that sepsis-produced HS fragments were capable of augmenting FGFR1 activation. These human-derived fragments augmented FGFR1 signaling in a manner consistent with full-length HS (Figure 7C). In contrast, HS fragments collected from the plasma of patients without sepsis with pneumonia had minimal impact on

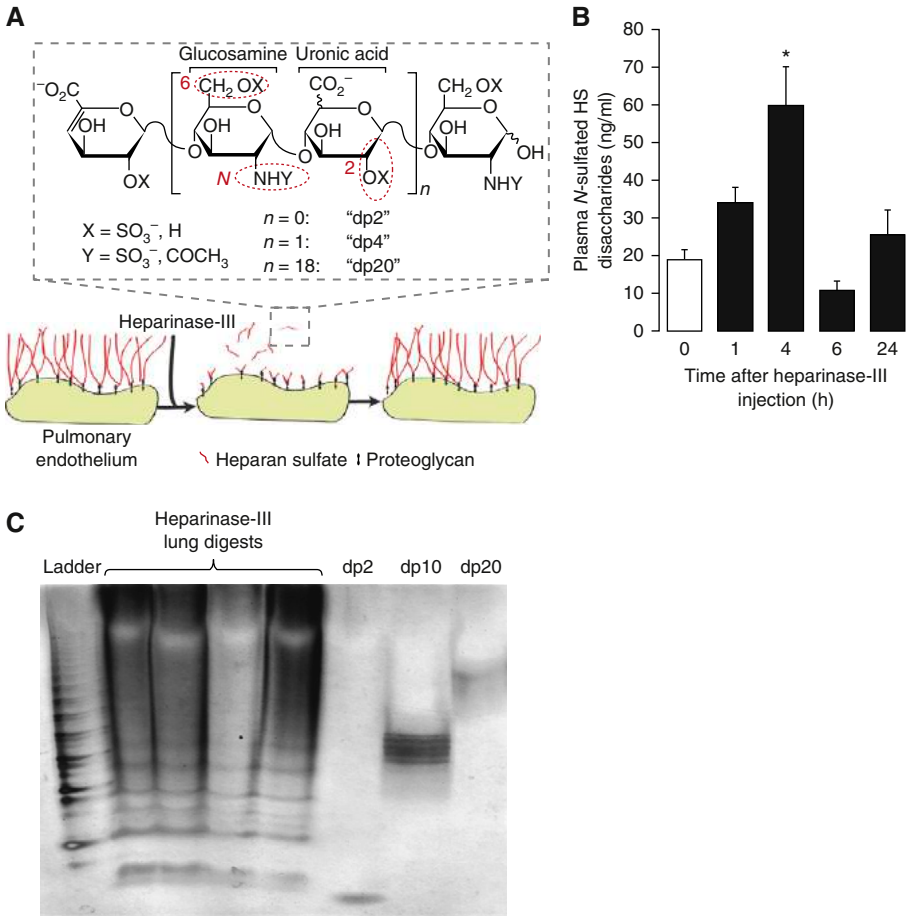

Figure 4. Structural characteristics of HS fragments released during heparinase-III–mediated ESL degradation. (*A*) HS is a polymer of repeating disaccharide units (with size quantified as degree of polymerization [dp]) that can be sulfated at 2-*O*, 6-*O*, and/or *N*-positions. *n*, number of repeats. (*B*) Heparinase-III treatment (1 unit intravenously) is associated with increased plasma *N*-sulfated HS, as measured by mass spectrometry. $^{*}P < 0.05$ compared with time = 0; $n > 3$ per group. (*C*) Heparinase-III treatment cuts lung HS in low-sulfation domains (X and Y are primarily hours and OCCH3, per *A*) yielding a range of fragment sizes, predominantly six saccharides (dp6) or larger, where X and Y (*A*) are primarily $SO3^{-}$. Heparinase-digested heparin ladder (*left*) shows disaccharides of all dp values found in heparin, and purified heparin dp2, dp10, and dp20 fragments (*right*) serve as size standards of gel electrophoresis. All graphs demonstrate mean values (±SE).

FGFR1c signaling (Figure E8), likely reflecting their undersulfated state (8). Taken together, these findings indicate that the delayed ESL reconstitution observed after CLP is not due to an inability of circulating HS fragments (released during septic ESL degradation) to activate FGFR1, but rather reflects the downstream absence of endothelial FGFR1 expression during sepsis (Figure 7D).

Discussion

This study identifies the endogenous mechanisms driving reconstitution of a degraded ESL. We found that nonseptic (i.e., heparinase-III–mediated) ESL degradation was followed by a rapid induction of endothelial FGFR1 expression, triggering homeostatic, EXT1-mediated pulmonary ESL reconstitution. ESL repair after heparinase-III was additionally promoted by the release of *N*-sulfated HS oligosaccharides capable of activating FGF2–FGFR1 signaling. Rapid induction of ESL repair by the very products of ESL degradation is biologically efficient, reflecting the critical importance of an intact ESL to endothelial homeostasis. In contrast to heparinase-III, CLP-mediated ESL degradation was associated with loss of reparative endothelial FGFR1 expression and, accordingly, delayed ESL reconstitution. However, HS fragments released during septic ESL degradation maintained FGFR1-promoting activity, indicating that septic suppression of ESL recovery occurs downstream of HS/FGF2 (Figure 7D). Taken together, these findings suggest that sepsis may cause vascular injury via not only ESL degradation, but also suppressed FGFR1/EXT1–mediated ESL recovery.

Our investigations (Figures 1–2, 4) of the mechanisms governing pulmonary ESL reconstitution are largely derived from a nonseptic model of heparinase-III (a bacterial HS–specific glucuronosyl lyase) –mediated pulmonary ESL degradation. We have previously demonstrated that sepsis is characterized by similarly rapid pulmonary ESL degradation by endothelial heparanase, a mammalian HS–specific glucuronosyl hydrolase (3). Heparinase-III (also known as heparitinase) and heparanase have been shown to act similarly upon matrix HS, releasing biologically active HS fragments (25). However, heparinase-III–mediated ESL degradation was insufficient to induce pulmonary vascular leak *in vivo* (Figure 1E) (26), whereas heparanase-mediated ESL degradation during sepsis directly contributed to lung edema and inflammation (3). These differences in the physiologic consequence of ESL degradation can be potentially explained by a concomitant loss of reparative HS biosynthetic enzymes (e.g., EXT1) during sepsis (Figures 1G and 1H), leading to a prolonged suppression of ESL integrity (Figure 1F). Indeed, heparinase-III treatment was able to induce lung edema at 24 hours only if subsequent HS biosynthesis was pharmacologically inhibited (Figure 1E).

Our work (Figure 2) specifically identifies endothelial FGFR1 as a critical regulator of EXT1 induction and homeostatic pulmonary ESL reconstitution. Endothelial FGFR signaling is an important mediator of vascular repair, with previous studies of Tie2Cre-*Fgfr1/2* knockout mice demonstrating impaired retinal microvascular responses to injury (7). Although these mice are characterized by endothelial loss of both FGFR1 and FGFR2, the relative absence of FGFR2 expression in the pulmonary microvascular endothelium (as demonstrated in Figure E2, and via analysis of publically available RNA

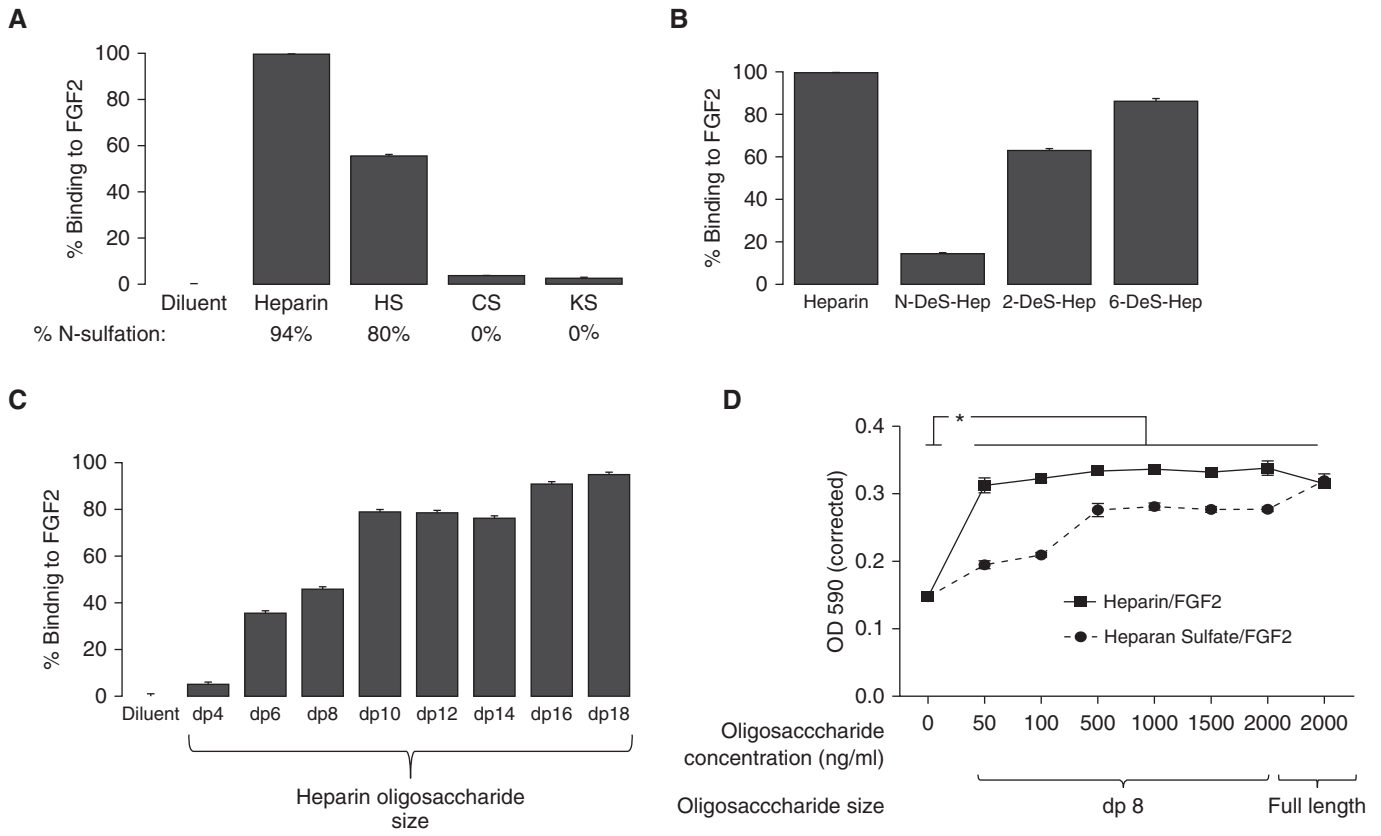

Figure 5. *N*-sulfated HS fragments can bind FGF2 and promote FGFR1c activation. Surface plasmon resonance studies revealed that highly *N*-sulfated glycosaminoglycans (such as HS or heparin [*A*]) readily bind FGF2 in an *N*-sulfation- (*B*) and size-dependent fashion (*C*). CS, chondroitin sulfate; KS, keratin sulfate. All group differences in (*A*–*C*) are statistically significant ($P < 0.05$). (*D*) HS or heparin octasaccharides augment FGF2 (5 nmol/L) activation of FGFR1c (the endothelial-expressed FGFR1 isoform), as demonstrated by increased growth/survival of FGFR1c-expressing BaF3 cells (*$P < 0.05$ for each concentration of heparin or HS, compared with oligosaccharide-unexposed control). Full-length (>dp18) heparin or HS serve as a positive control. $n > 3$ for all groups. OD 590, optical density at 590 nm. All graphs demonstrate mean values (±SE).

sequencing data [17]) provides reassurance that our pulmonary EXT1 findings are largely FGFR1-driven.

Although we observed that sepsis is associated with loss of (ESL-reparative) FGFR1 expression, the mechanisms responsible for this suppression remain uncertain. One potential mediator of septic FGFR1 down-regulation is miR-16, an endothelial miR that decreases FGFR1 expression and suppresses angiogenesis (19). Previous reports have observed increased plasma miR-16 in human and murine sepsis (20, 21). Surprisingly, we found little evidence of pulmonary miR-16 induction at time points coincident with loss of pulmonary FGFR1 (Figure 3C). Furthermore, inhibition of miR-16 failed to prevent the septic loss of pulmonary EXT1 expression (Figure 3D). The apparent miR-16 independence of septic suppression of ESL recovery is compatible with the observation that elevated plasma miR-16, despite being a marker of sepsis, is correlated with improved septic outcomes in humans (27). The mechanisms governing loss of endothelial FGFR1 during sepsis will require further study.

In addition to identifying FGFR1 expression as a mediator of ESL repair, our work highlights the importance of ESL-derived HS fragments in promoting FGFR1 activation. Although others have reported circulating HS as a biomarker of ESL degradation, the biological function of these oligosaccharides has been largely relegated to serving as a damage-associated molecular pattern, with less attention to impact on other signaling pathways. When anchored to cell-surface proteoglycans, HS may function as a *cis*-activating coreceptor for growth factor ligand–receptor interaction (10). Our findings suggest that endothelial growth factor signaling can be paradoxically augmented by HS degradation, provided that the products of this degradation (HS oligosaccharides) are of sufficient size (>dp6) and sulfation (*N*-sulfated) to bind soluble FGF2 and activate FGF2–FGFR1 signaling. This sulfation requirement for growth factor activation suggests that HS degradation might release cryptic, highly sulfated HS domains not participatory in *cis* activation of growth factor signaling. Alternatively, released HS oligosaccharides might access basolateral growth factor receptors otherwise unengaged by apical HS proteoglycans. Determination of the geographic localization of these interactions will require future development of highly sensitive glycosaminoglycan-labeling and -sequencing techniques.

The critical necessity of ESL integrity to the maintenance of vascular physiology suggests that there likely exist additional

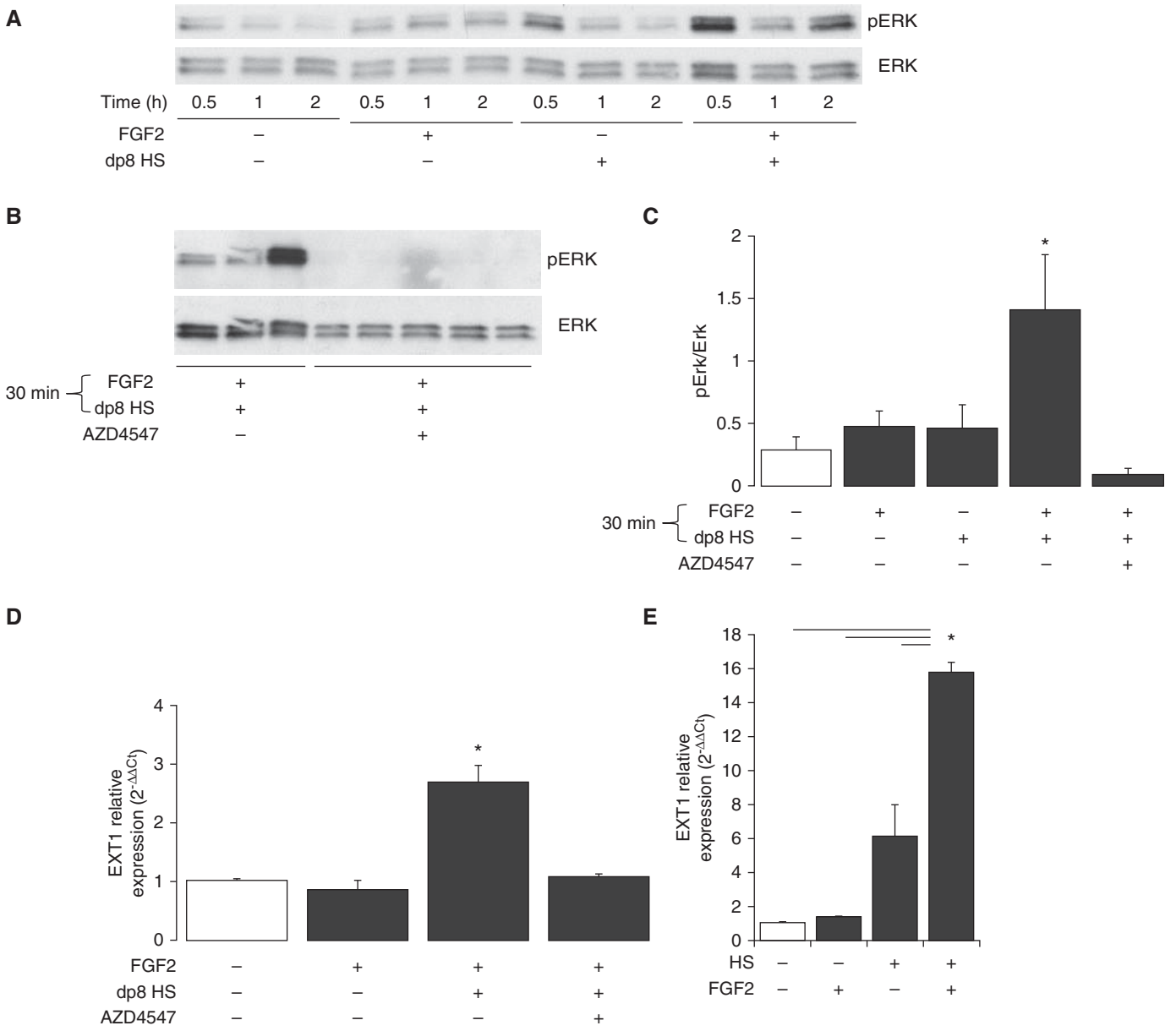

Figure 6. HS-FGF2 activates endothelial growth factor signaling and EXT1 expression. (*A*) dp8 HS (0.5 μg/ml) and FGF2 (5 ng/ml) activated growth factor signaling in HPMEC-ST1.6R cells, as measured by extracellular signal–regulated kinase (ERK) phosphorylation (pERK). (*B*) Pretreatment (12 h, 20 nmol/L) with the FGFR1 inhibitor, AZD4547, confirmed that ERK phosphorylation (induced by 30 min dp8 HS/FGF2) was FGFR dependent. (*C*) Densitometry quantification of 30-minute FGF2/dp8 HS treatments in *A* and *B*. (*D*) dp8 HS and FGF2 (3-h treatment) of HPMEC-ST1.6R cells similarly induced EXT1 mRNA expression in an FGFR-dependent fashion. (*E*) Similar induction of EXT1 expression was noted in primary mouse lung microvascular endothelial cells treated with HS (5 μg/ml) and FGF2 (20 ng/ml) for 5 hours. $n > 3$ for all groups; $^*P < 0.05$. All graphs demonstrate mean values (±SE).

systems of glycosaminoglycan biosynthesis and ESL recovery complementary to FGF2/FGFR1 signaling. Indeed, inhibition of FGFR1 signaling did not completely suppress EXT1 expression or ESL recovery 24 hours after heparinase-III (Figure 2), and this partial suppression of ESL recovery was only capable of inducing lung edema after AZD4547-mediated FGFR1 inhibition (potentially suggesting compensatory lung-protective mechanisms in Tie2Cre: *Fgfr1/2*$^{f/f}$ mice; Figure E4). There is further need to study alternative mechanisms of EXT1 induction, and how these mechanisms may be impacted during sepsis. Our work specifically highlights the complexity of EXT1 regulation: the observed rise in protein expression before a statistically significant rise in gene transcription suggests that rapid changes in HS biosynthesis may occur at the post-translational level, potentially via prevention of EXT1 proteosomal degradation. Indeed, the *in vivo* regulation of heparan synthesis and sulfation remains uncertain, and is the focus of active investigation (28).

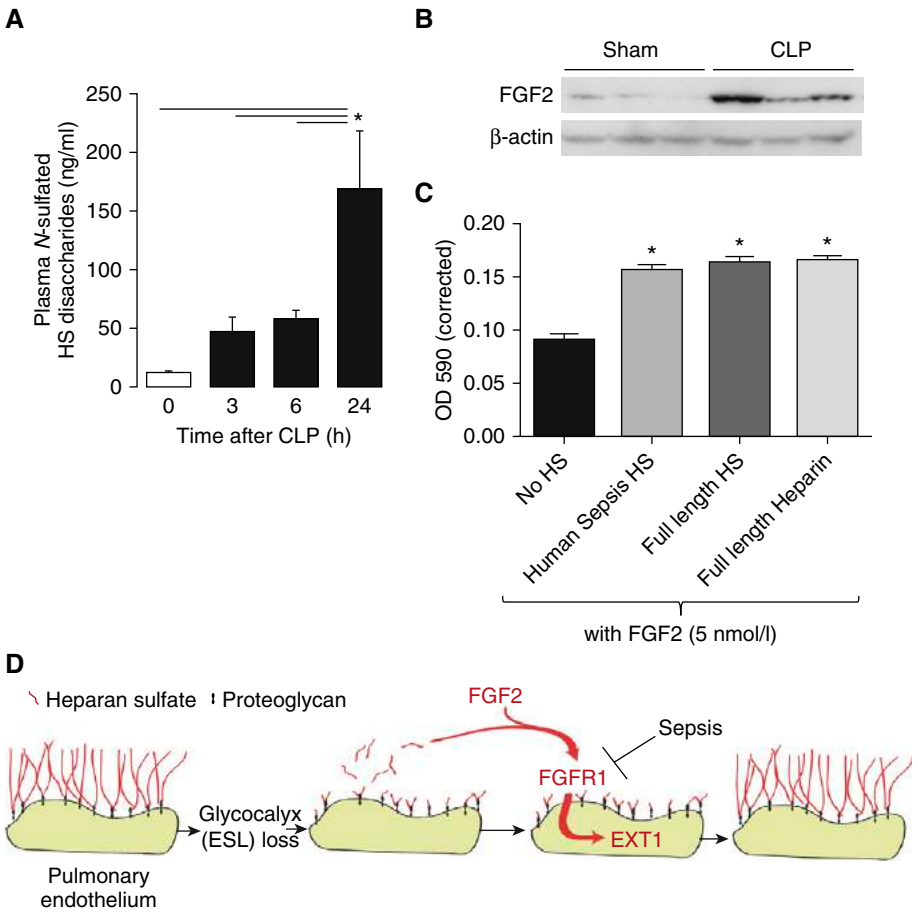

Figure 7. Septic loss of HS-FGF2-FGFR1 signaling occurs downstream of HS-FGF2. CLP was associated with increased plasma *N*-sulfated HS (*A*) and pulmonary FGF2 ([*B*] 24 h after CLP). (*C*) HS fragments (250 ng/ml) pooled from the plasma of patients with sepsis were capable of activating FGFR1c in FGF2- (5 nmol/L) treated BaF3 cells. (*D*) Proposed pathway of ESL reconstitution. As septic plasma HS fragments remain capable of activating FGF2/FGFR1, impairment of FGFR1-mediated ESL reconstitution during sepsis likely occurs owing to loss of endothelial FGFR1 expression. $n > 3$ per group; $^*P < 0.05$. All graphs demonstrate mean values (±SE).

Consistent with the lungs' functional susceptibility to the consequences of ESL loss (e.g., hypoxia arising from pulmonary edema and inflammation), pulmonary ESL recovery after heparinase-III occurred much more rapidly (<24 h) than cremasteric ESL recovery after heparinase-III (5 d [5]). Notably, even the slowed pace of pulmonary ESL recovery in CLP-treated mice (3 d; Figure 1F) was more rapid than that of the cremasteric ESL in healthy animals. Pulmonary ESL recovery is so highly prioritized that it is initiated before the resolution of systemic illness, as CLP-treated mice typically demonstrate continued signs of illness (lethargy, piloerection) at 48 hours, a time point at which ESL reconstitution has already begun (Figure 1F). The mechanisms responsible for these organ-specific differences in the pace of ESL recovery require further investigation. Although these may be partially explained by tissue-specific differences in FGFR signaling (as demonstrated by the differential expression of FGFR2 in pulmonary [Figure E2] and systemic endothelium [7]), other influences, such as organ-specific differences in vascular shear stress waveforms (with tidal variability occurring in the inflating/deflating lung) may contribute to the rapidity of pulmonary HS synthesis (29).

In summary, this work represents the first investigation of the endogenous mechanisms underlying homeostatic pulmonary ESL reconstitution. Furthermore, this report identifies that FGFR1 serves as a critical mediator of ESL repair and is suppressed during sepsis. Our work raises numerous additional mechanistic questions, the pursuit of which promises to provide greater insight into ESL physiology during health and disease. ■

Author disclosures are available with the text of this article at www.atsjournals.org.

Acknowledgments: The authors thank Dr. David Ornitz (Washington University in St. Louis, St. Louis, MO) for generously providing BaF3 cells and Tie2Cre:*Fgfr1/2*$^{f/f}$ mice and for providing technical advice. The authors also thank Dr. Ronald Unger (University of Mainz, Mainz, Germany) for providing HPMEC-ST1.6R cells.

References

1. Schmidt EP, Kuebler WM, Lee WL, Downey GP. Adhesion molecules: master controllers of the circulatory system. *Compr Physiol* 2016;6: 945–973.
2. Haeger SM, Yang Y, Schmidt EP. Heparan sulfate in the developing, healthy, and injured lung. *Am J Respir Cell Mol Biol* 2016;55:5–11.
3. Schmidt EP, Yang Y, Janssen WJ, Gandjeva A, Perez MJ, Barthel L, Zemans RL, Bowman JC, Koyanagi DE, Yunt ZX, *et al*. The pulmonary endothelial glycocalyx regulates neutrophil adhesion and lung injury during experimental sepsis. *Nat Med* 2012;18:1217–1223.
4. Lygizos MI, Yang Y, Altmann CJ, Okamura K, Hernando AA, Perez MJ, Smith LP, Koyanagi DE, Gandjeva A, Bhargava R, *et al*. Heparanase mediates renal dysfunction during early sepsis in mice. *Physiol Rep* 2013;1:e00153.
5. Potter DR, Jiang J, Damiano ER. The recovery time course of the endothelial cell glycocalyx in vivo and its implications in vitro. *Circ Res* 2009;104:1318–1325.
6. Giantsos-Adams KM, Koo AJ, Song S, Sakai J, Sankaran J, Shin JH, Garcia-Cardena G, Dewey CF Jr. Heparan sulfate regrowth profiles under laminar shear flow following enzymatic degradation. *Cell Mol Bioeng* 2013;6:160–174.
7. Oladipupo SS, Smith C, Santeford A, Park C, Sene A, Wiley LA, Osei-Owusu P, Hsu J, Zapata N, Liu F, *et al*. Endothelial cell FGF signaling is required for injury response but not for vascular homeostasis. *Proc Natl Acad Sci USA* 2014;111:13379–13384.
8. Schmidt EP, Li G, Li L, Fu L, Yang Y, Overdier KH, Douglas IS, Linhardt RJ. The circulating glycosaminoglycan signature of respiratory failure in critically ill adults. *J Biol Chem* 2014;289:8194–8202.

9. Yang Y, Yang G, Schmidt EP. *In vivo* measurement of the mouse pulmonary endothelial surface layer. *J Vis Exp* 2013;(72):e50322.
10. Goetz R, Mohammadi M. Exploring mechanisms of FGF signalling through the lens of structural biology. *Nat Rev Mol Cell Biol* 2013;14: 166–180.
11. Sterner E, Meli L, Kwon SJ, Dordick JS, Linhardt RJ. FGF–FGFR signaling mediated through glycosaminoglycans in microtiter plate and cell-based microarray platforms. *Biochemistry* 2013;52: 9009–9019.
12. Chappell D, Jacob M, Rehm M, Stoeckelhuber M, Welsch U, Conzen P, Becker BF. Heparinase selectively sheds heparan sulphate from the endothelial glycocalyx. *Biol Chem* 2008;389:79–82.
13. Sarrazin S, Lamanna WC, Esko JD. Heparan sulfate proteoglycans. *Cold Spring Harb Perspect Biol* 2011;3:a004952.
14. Nigro J, Wang A, Mukhopadhyay D, Lauer M, Midura RJ, Sackstein R, Hascall VC. Regulation of heparan sulfate and chondroitin sulfate glycosaminoglycan biosynthesis by 4-fluoro-glucosamine in murine airway smooth muscle cells. *J Biol Chem* 2009;284:16832–16839.
15. Cedeno-Laurent F, Opperman MJ, Barthel SR, Hays D, Schatton T, Zhan Q, He X, Matta KL, Supko JG, Frank MH, *et al*. Metabolic inhibition of galectin-1–binding carbohydrates accentuates antitumor immunity. *J Invest Dermatol* 2012;132:410–420.
16. Okada M, Nadanaka S, Shoji N, Tamura J, Kitagawa H. Biosynthesis of heparan sulfate in EXT1-deficient cells. *Biochem J* 2010;428: 463–471.
17. Zhang LQ, Cheranova D, Gibson M, Ding S, Heruth DP, Fang D, Ye SQ. RNA-seq reveals novel transcriptome of genes and their isoforms in human pulmonary microvascular endothelial cells treated with thrombin. *PLoS One* 2012;7:e31229.
18. Gavine PR, Mooney L, Kilgour E, Thomas AP, Al-Kadhimi K, Beck S, Rooney C, Coleman T, Baker D, Mellor MJ, *et al*. AZD4547: an orally bioavailable, potent, and selective inhibitor of the fibroblast growth factor receptor tyrosine kinase family. *Cancer Res* 2012;72: 2045–2056.
19. Chamorro-Jorganes A, Araldi E, Penalva LO, Sandhu D, Fernández-Hernando C, Suárez Y. MicroRNA-16 and microRNA-424 regulate cell-autonomous angiogenic functions in endothelial cells via targeting vascular endothelial growth factor receptor-2 and fibroblast growth factor receptor-1. *Arterioscler Thromb Vasc Biol* 2011;31: 2595–2606.
20. Wang H, Zhang P, Chen W, Feng D, Jia Y, Xie LX. Evidence for serum miR-15a and miR-16 levels as biomarkers that distinguish sepsis from systemic inflammatory response syndrome in human subjects. *Clin Chem Lab Med* 2012;50:1423–1428.
21. Wu SC, Yang JC, Rau CS, Chen YC, Lu TH, Lin MW, Tzeng SL, Wu YC, Wu CJ, Hsieh CH. Profiling circulating microRNA expression in experimental sepsis using cecal ligation and puncture. *PLoS One* 2013;8:e77936.
22. Colbert JF, Schmidt EP. Endothelial and microcirculatory function and dysfunction in sepsis. *Clin Chest Med* 2016;37:263–275.
23. Guzy RD, Stoilov I, Elton TJ, Mecham RP, Ornitz DM. Fibroblast growth factor 2 is required for epithelial recovery, but not for pulmonary fibrosis, in response to bleomycin. *Am J Respir Cell Mol Biol* 2015; 52:116–128.
24. Krump-Konvalinkova V, Bittinger F, Unger RE, Peters K, Lehr HA, Kirkpatrick CJ. Generation of human pulmonary microvascular endothelial cell lines. *Lab Invest* 2001;81:1717–1727.
25. Kato M, Wang H, Kainulainen V, Fitzgerald ML, Ledbetter S, Ornitz DM, Bernfield M. Physiological degradation converts the soluble syndecan-1 ectodomain from an inhibitor to a potent activator of FGF-2. *Nat Med* 1998;4:691–697.
26. Yang Y, Schmidt EP. The endothelial glycocalyx: an important regulator of the pulmonary vascular barrier. *Tissue Barriers* 2013;1:1.
27. Wang H, Zhang P, Chen W, Feng D, Jia Y, Xie L. Serum microRNA signatures identified by Solexa sequencing predict sepsis patients' mortality: a prospective observational study. *PLoS One* 2012;7: e38885.
28. Zhang X, Wang F, Sheng J. "Coding" and "decoding": hypothesis for the regulatory mechanism involved in heparan sulfate biosynthesis. *Carbohydr Res* 2016;428:1–7.
29. Koo A, Dewey CF Jr, García-Cardeña G. Hemodynamic shear stress characteristic of atherosclerosis-resistant regions promotes glycocalyx formation in cultured endothelial cells. *Am J Physiol Cell Physiol* 2013;304:C137–C146.